Supplementary Information

Efficient single-emitter plasmonic patch antenna fabrication by deterministic in situ optical lithography using spatially modulated light

Amit Raj Dhawan[1,2,4], Michel Nasilowski[3], Zhiming Wang[1], Benoît Dubertret[3], Agnès Maître[2*]

[1] Institute of Fundamental and Frontier Sciences, University of Electronic Science and Technology of China, Chengdu 610054, People's Republic of China
[2] Sorbonne Universités, UPMC Univ Paris 06, UMR 7588, Institut de NanoSciences de Paris (INSP), Paris F-75005, France
[3] Laboratoire de Physique et d'Etude des Matériaux, ESPCI-ParisTech, PSL Research University, Sorbonne Université UPMC Univ Paris 06, CNRS, 10 rue Vauquelin 75005 Paris, France
[4] Department of Materials, University of Oxford, Parks Road, Oxford, OX1 3PH, UK

*Corresponding author. Email: agnes.maitre@insp.upmc.fr, Telephone: +33 1 44 27 42 172

Contents

S1 Quantum dot synthesis

The CdSe/CdS core/shell colloidal quantum dots (QDs) were fabricated firstly by growing the CdSe core using the method illustrated in references [1] and [2]. Then the CdS monolayers were grown over the core by slow injection to obtain the desired thickness.

S1.1 CdSe core

750 µl of 0.5 M cadmium oleate [$Cd(C_{18}H_{34}O_2)_2$], 1.5 ml of TOPO [trioctylphosphine oxide, $[CH_3(CH_2)_7]_3PO$], 1.5 ml of octadecene [$C_{18}H_{36}$] were mixed in a 100 ml flask with three necks, and degassed for 3 hours at 70℃. Ar gas was let into the flask and the solution was heated from 20℃ to 300℃. As the temperature reached 300℃, 4 ml of trioctylphosphine selenide [TOPSe, $(C_8H_{17})_3P{=}Se$] was added promptly, and then 3 ml oleamine or oleylamine [$C_{18}H_{35}NH_2$] was injected into the flask, and the mixture was annealed for 8 minutes as the CdSe cores were being synthesized. To stop the chemical synthesis of the cores, the flask is brought to room-temperature. For enhancing the stability of the cores, 0.1 ml of oleic acid [$C_{18}H_{34}O_2$] was injected into the flask. The precipitation of the cores was done by adding ethanol [C_2H_5OH] to the solution. After collecting just the precipitated CdSe cores, they were dispersed in 5 ml of octadecane [$C_{18}H_{38}$].

S1.2 CdSe shell

The dispersion of CdSe cores in octadecane was added into a three-neck flask with 50 mg of cadmium. The contents of the flask were degassed at 70℃ for 45 minutes under Ar flow. A mixture of 1 ml of oleylamine, 1 ml of 0.5 M cadmium oleate, and 5 ml of 8.1 M solution of sulphur in octadecene was prepared. 2 ml of this solution was injected into the flask at 2 ml/hour, and the remaining 3 ml of this solution was added at 18 ml/hour. The contents of the flask were heated for 10 minutes at 300℃. Then the flask was brought to room-temperature and the CdSe/CdS core/shell nanocrystals were precipitated using ethanol, and were dispersed in 5 ml of hexane [C_6H_{14}]. The ligands that hold the QD in a non-polar solvent (such as hexane or toluene) comprises a carbon chain of 18 atoms, which is terminated by either COO^- or NH_2. In this colloid, the alkyl chain attaches to the solvent, and the COO^- and NH_2 attach to the QD.

S2 Quantum dot emission

The low power required to excite the antenna of Figure 5 in the paper is highlighted when compared to the case where a typical QD is excited without an antenna. Figure S1 shows the response of a typical QD under varying excitation power. A QD placed on a silica window was covered with a 100 nm thick layer of poly(methyl methacrylate) (PMMA) and was viewed confocally using a 0.8NA air objective and a 405 nm pulsed laser (50 ps pulse width) at 2.5 MHz.

Note that the power in the figure below is in μW, whereas in Figure 5, it is nW. This demonstrates how the positioning of an antenna over a QD can increase its effective absorption cross-section. We find the absorption cross-section (σ_{abs}) of the QD of Figure S1 to be 4.8×10^{-14} cm^2. The photon rate has been fit with similar trends as discussed in the paper: $1 - e^{-\beta P}$ for the first part, and P^{α} for the nonlinear part, where P is the average laser power. In this case, $\beta = 10.2\,\mu W^{-1}$ and $\alpha = 4.3$. All the antennas discussed in this paper used QDs from the same batch and showed $\sigma_{abs} \approx 10^{-14}$ cm^2.

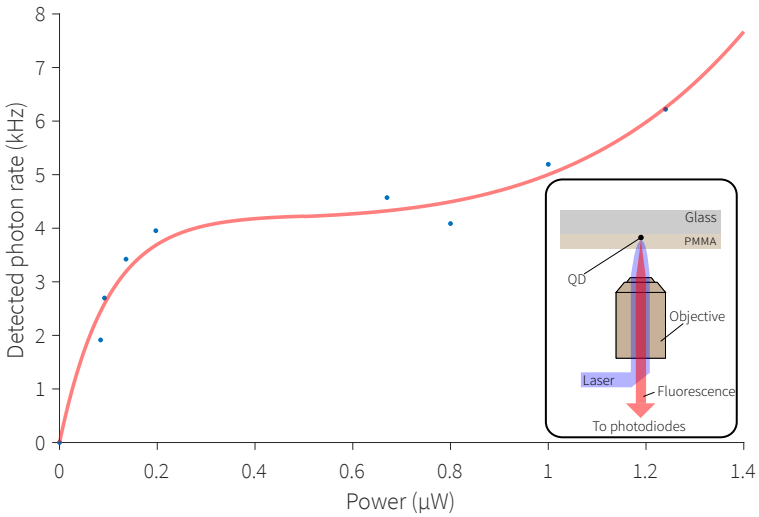

Figure S1 *QD emission*

QD photon rate was recorded as the power of the laser was increased—measured (blue dots) and fit (red curve). The inset illustrates the measurement scheme.

S3 Absorption cross-section

The exciton absorption cross-section can be calculated from the first part of the power versus detected photon rate curve before the onset of multexciton emission as shown in Figure 5 of the paper. Exciton emission can be modelled by a two-level system (Figure S2), where a bound electron-hole pair (exciton) created by absorbing a photon can recombine to generate a photon. The recombination can be radiative or non-radiative.

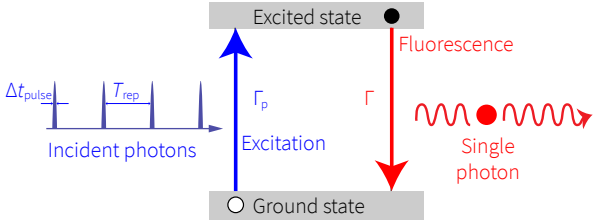

Figure S2 *Two level system*

Consider a system that is being excited by a pulsed laser of pulse width Δt_{pulse}, repetition rate f_{rep}, and wavelength λ, where each pulse pumps the system at a pumping rate of Γ_p, and after excitation the system relaxes by exciton recombination with Γ. The occupational probabilities of the ground and excited state at any given time t are $p_0(t)$ and $p_1(t)$, resp., and can be obey the following:

$$\frac{dp_0}{dt} = -\Gamma_p p_0(t) + \Gamma p_1(t) \tag{1}$$

$$\frac{dp_1}{dt} = \Gamma_p p_0(t) - \Gamma p_1(t) \tag{2}$$

The total probability at any instant $p_0(t) + p_1(t) = 1$. Using the equations above and the initial condition that the system is in the ground state before the arrival of the pulse

$$p_1(t = -\Delta t_{pulse}) = 0 \tag{3}$$

we find that

$$p_1(t) = \left(\frac{\Gamma_p}{\Gamma_p + \Gamma}\right)\left[1 - e^{-(\Gamma_p+\Gamma)\Delta t_{pulse}}\right] e^{-\Gamma t} \tag{4}$$

The pumping rate in each pulse Γ_p, the power in each peak P_{peak} are related to the average pumping rate $\langle\Gamma_p\rangle$ and the average laser power P (measured by the power meter) as:

$$\frac{\Gamma_p}{P_{peak}} = \frac{\langle\Gamma_p\rangle}{P} \tag{5}$$

and

$$P = P_{peak} \times \Delta t_{pulse} \times f_{rep} \tag{6}$$

In the process of excitation of the emitter during a laser pulse, Γ_p is related to P_{peak} through the absorption cross-section σ_{abs}:

$$\Gamma_P = \frac{\sigma_{abs}\, P_{peak}}{A_{spot}\, hc/\lambda} \tag{7}$$

where A_{spot} is the area of the incident laser spot and hc/λ is the incident photon energy (h: Planck's constant, c: speed of light in vacuum, λ: laser wavelength).

The instantaneous photon rate $\Gamma_D(t)$ is defined as:

$$\begin{aligned}\Gamma_D(t) &\equiv p_1(t)\Gamma_{rad}\,\eta_o \\ &= p_1(t)\Gamma\,\eta_e\eta_o\end{aligned} \tag{8}$$

where η_e is the quantum efficiency of the emitter, η_o is the detection efficiency of the optical setup, Γ is the emitter decay rate, and Γ_{rad} is the radiative decay rate of the emitter. By integrating $\Gamma_D(t)$ over a period ($T_{rep} = 1/f_{rep}$), we find that the average detection rate $\langle\Gamma_D\rangle$ is:

$$\langle\Gamma_D\rangle = \left(\frac{\Gamma_p}{\Gamma_p + \Gamma}\right)\left[1 - e^{-(\Gamma_p+\Gamma)\Delta t_{pulse}}\right] \eta_e\, \eta_o\, f_{rep} \tag{9}$$

Figure S3 shows the evolution of $\langle\Gamma_D\rangle$ with Γ_p.

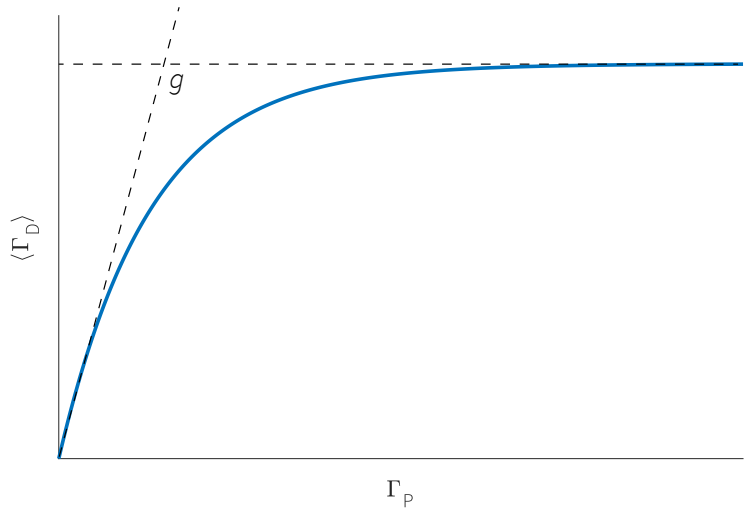

Figure S3 *Detected photon rate*

Under low pumping, where $\Gamma_p \ll \Gamma$ and $\Gamma_p \, \Delta t_{pulse} \ll 1$, we find

$$\langle \Gamma_D \rangle = \eta_e \, \eta_o \, \langle \Gamma_p \rangle \tag{10}$$

Under high pumping, where $\Gamma_p \gg \Gamma$ and $\Gamma_p \, \Delta t_{pulse} \gg 1$

$$\langle \Gamma_D \rangle = \eta_e \, \eta_o \, f_{rep} \tag{11}$$

From above equations we find that at the transition from low to high pumping (point g in Figure S3)

$$\sigma_{abs} = \frac{hc}{\lambda} A_{spot} \, f_{rep} \, \frac{1}{P_g} \tag{12}$$

where P_g is the power at point g in Figure S3. The above equation is equivalent to

$$\sigma_{abs} = \frac{hc}{\lambda} A_{spot} \, f_{rep} \, \beta \tag{13}$$

Here β is deduced from the fit $\gamma(1-e^{-\beta P})$ that is used for fitting the first part of the curve of $\langle \Gamma_D \rangle$ vs P (Figure S1).

References

[1] X. Peng, J. Wickham, and A. P. Alivisatos, "Kinetics of II-VI and III-V Colloidal Semiconductor Nanocrystal Growth: "Focusing" of Size Distributions," *Journal of the American Chemical Society*, vol. 120, no. 21, pp. 5343–5344, Jun. 1998. [Online]. Available: http://doi.org/10.1021/ja9805425

[2] X. Peng, L. Manna, W. Yang, J. Wickham, E. Scher, A. Kadavanich, and A. P. Alivisatos, "Shape control of CdSe nanocrystals," *Nature*, vol. 404, no. 6773, pp. 59–61, Mar. 2000. [Online]. Available: http://doi.org/10.1038/35003535